

PREDICTIONS OF THERMAL COMFORT AND POLLUTANT DISTRIBUTIONS FOR A
THERMOSTATICALLY-CONTROLLED, AIR-CONDITIONED, PARTITIONED ROOM:
NUMERICAL RESULTS AND ENHANCED GRAPHICAL PRESENTATION

Dr. Mark White
Senior Research Engineer
Pacific Northwest Laboratory
Richland, Washington^a

Dr. L. Loren Eyler
Senior Research Engineer
Pacific Northwest Laboratory
Richland, Washington

ABSTRACT

An index of local thermal comfort and pollutant distributions have been computed with the TEMPEST computer code, in a transient simulation of an air-conditioned enclosure with an incomplete partition. This complex three-dimensional air-conditioning problem included forced ventilation through inlet vents, flow through a partition, remote return air vents, an infiltration source, a pollutant source, and a thermostatically controlled air-conditioning system. Five forced ventilation schemes that varied in vent areas and face velocities were simulated. Thermal comfort was modeled as a three-dimensional scalar field dependent on the fluid velocity and temperature fields; where humidity, activity levels, and clothing were considered constants. Pollutant transport was incorporated through an additional constituent diffusion equation. Six distinct graphics techniques for the visualization of the three-dimensional data fields of air velocity, temperature, and comfort index were tested.

INTRODUCTION

Forced ventilation systems in commercial and residential buildings are designed to provide a comfortable environment to the occupants and to maintain the indoor air quality. Thermal comfort has previously been shown (ASHRAE 1985) to depend on at least six factors: air temperature, air speed, mean radiant temperature, humidity, clothing insulation, and activity level. If we assume values for clothing insulation and activity levels, the remaining four factors that influence thermal comfort are generally subject to environmental control and can vary locally within the volume of a single room. It is possible that the volume averaged values of the four environmental factors would predict acceptable thermal comfort levels for the room, while local zones within the room feel uncomfortable.

The presence of pollutants in buildings can impact the occupants in numerous ways from minor annoyance, to hindering work performance, or representing a health hazard. As a result, there is currently a substantial interest in the ability to predict thermal comfort and pollutant distributions, pollutant motion, and pollutant persistence as a function of ventilation system design and operation.

While the methodologies for predicting thermal comfort and pollutant distribution continue to improve, there remains the issue of communicating the results to the design community. Enormous amounts of primitive and conditioned data can be produced in predicting spatial and temporal variations in thermal comfort and pollutant distributions. Scanning reams of computer output in tabular form should be considered unacceptable, except for research or algorithm development purposes. Moreover, the conventional formats in the building sciences for presenting results, such as, graphs, tables, and diagrams, have limitations in communicating multidimensional and multicomponent information.

This paper reports the results from a finite-difference approach to the solution of the Navier-Stokes and constituent diffusion equations, and its application to the simulation of an air-conditioned building with a pollutant source. The model building was a three-dimensional, two room enclosure, which was divided by an incomplete partition with a doorway connecting the two rooms. A thermostatically controlled air-conditioning ventilation system was modeled that offset the relatively hot thermal boundary conditions. Parametric cases that differed in ventilation flow rates, infiltration rates through a curtained window, and vent areas were computed. A pollutant 10% less dense than the room air was included. The pollutant source was assumed to be uniformly distributed over the ceiling region of one room, at constant source strength.

^a Operated by Battelle Memorial Institute for the U.S. Department of Energy under Contract DE-AC06-76RLO 1830.

We used the results from the air-conditioning simulation problem for the development and investigation of visualization techniques of scalar and vector fields. Six distinct graphics presentation techniques were investigated with the aim of enhancing the visualization of the three-dimensional data fields of air velocity, temperature, and comfort index through the use of color, motion, and shading on a computer monitor.

NAVIER-STOKES MODEL

The Navier-Stokes equations that describe mass, momentum, and energy transport were solved in the present investigation with the TEMPEST (Trent, Eyster, and Budden 1989) computer code. TEMPEST is a three-dimensional, time-dependent computer program for hydrothermal analysis, which uses a finite-difference approach to solve the transient Navier-Stokes equations. Constituent transport is accommodated by solving additional partial differential equations for mass diffusion. Thermodynamic state relationships are required along with other tabular data for the definition of temperature-dependent material properties. TEMPEST does not solve the Navier-Stokes equations in their complete form, but rather an incompressible form subject to assumptions and/or restrictions. The primary assumption that concerns air flows characteristic of the building sciences (natural convection flows or combined forced and natural convection flows), is that the Boussinesq approximation holds.

The Boussinesq approximation is commonly used in natural convection simulations involving either liquids or gases. The principal simplification associated with the Boussinesq approximation is that the density terms of the Navier-Stokes equation are treated as constants except in the body force terms of the momentum equation. This approximation is reasonable provided that density changes are relatively small compared with the local fluid density. For building simulations of forced or natural convection flows the Boussinesq approximation is generally appropriate.

TEMPEST was designed to simulate in the subsonic regime; therefore, the viscous dissipation function has been eliminated from the energy conservation equation. Fluids are considered Newtonian. For laminar flow situations the incompressible form of the Navier-Stokes equations is solved directly. For turbulent flow, the Reynolds stresses are modeled through an effective viscosity and the turbulent thermal diffusivity through an effective thermal conductivity. The Prandtl-Kolmogorov hypothesis is

used to relate the effective viscosity to a velocity and a length scale. In this approach, transport equations for the turbulent kinetic energy and the dissipation of turbulent kinetic energy are solved to determine the effective turbulent viscosity.

The TEMPEST solution procedure is a semi-implicit, time marching finite-difference procedure with all governing equations solved sequentially. For each time step the momentum equations are solved explicitly and the pressure equations implicitly; temperature, turbulent kinetic energy, and dissipation of turbulent kinetic energy other scalar transport equations are solved using an implicit continuation procedure. For the present investigation, thermostat logic that controlled the forced air-conditioning ventilation cycling was incorporated into the code.

POLLUTANT TRANSPORT MODEL

The TEMPEST pollutant transport model is actually a mass transport model that incorporates the capability to accommodate up to nine constituents. The pollutant transport model is composed of: 1) input routines for constituent properties, boundary conditions that include time-dependent tables, and initial values; 2) mixture thermodynamic logic; 3) transport equation solution logic; and 4) output routines. As with the Navier-Stokes model certain limitations and assumptions are applicable to the mass transport model in TEMPEST.

The rate of species injection must remain relatively low when compared with the total room infiltration rates in order to conserve the constant system pressure assumptions required in the Navier-Stokes model. The model does not accommodate droplet/aerosol transport where slip occurs between the fluid and particulate. Condensation or phase change of one constituent cannot be accommodated. The concentration of the pollutant species must remain dilute because the $k-\epsilon$ turbulence model is dependent on the base component viscosity, and because the computation of molecular diffusivities for component mixtures has been omitted from the model.

With respect to the mixture thermodynamic logic for constituent transport, mixture values are computed for the density and specific heat. Gaseous constituents are treated as perfect gases. The transport equation logic for constituent transport in TEMPEST involves solving additional partial differential equations. The number of constituent transport equations depends on the number of species being modeled; one additional differential

diffusion equation for each mass specie. The mass diffusivity of a constituent is treated in one of several ways depending on input specifications. For laminar flow, the mass diffusivity equals the molecular diffusivity; whereas for turbulent flow, the mass diffusivity is dependent on turbulent viscosity and Schmidt number.

THERMAL COMFORT MODEL

Because it is inherently subjective, thermal comfort is a difficult parameter to quantify. Heat balance equations have been written for the human body that may be used to predict combinations of environmental factors, levels of activity, and clothing insulation that produce thermal comfort (ASHRAE 1985, Fanger 1967). Such heat balance equations, whether in functional, tabular, or graphic form, have utility for design purposes, but are inappropriate for predicting the divergence from a "comfortable" environment given an arbitrary set of environmental factors, level of activity, and clothing insulation. Fanger (1970, ASHRAE 1985), however, devised an index, entitled the "Predicted Mean Vote" (PMV), expressly designed for this purpose. PMV is a psychophysical index that reflects the thermal comfort sentiments of a large group of subjects. The index is scaled from -3 to 3, where the absolute value of the divergence of the index from 0 reflects the level of discomfort, either cold or hot, respectively. Fanger's PMV scale appears as:

- 3 = cold
- 2 = cool
- 1 = slightly cool
- 0 = neutral comfort
- +1 = slightly warm
- +2 = warm
- +3 = hot

The PMV thermal discomfort index is dependent on the four environmental factors of temperature, air velocity, humidity, and mean radiant temperature, for fixed values of the level of activity and clothing insulation. Fanger (1970) compiled a comprehensive table for predicting the PMV from the six dependent variables.

The thermal comfort model in TEMPEST is structured around the PMV table. Values for the clothing insulation in "clo" units ($0.155 \text{ m}^2 \text{ }^\circ\text{C/W}$), the relative humidity, and level of activity are assigned. With these parameters defined, three environmental variables remain that must be computed to determine the PMV: the temperature, air speed, and mean radiant temperature. In the subject version of the

TEMPEST thermal comfort model the mean radiant temperature is assumed equal to the air temperature. The local air temperature and speed used in the thermal comfort model are those computed from the Navier-Stokes model. This approach allows the combination of temperature and air speed to be expressed in terms of thermal comfort or discomfort as a single local quantity. If water vapor is declared as a constituent in the TEMPEST transport model, then the local humidity can be computed from the local air moisture content and temperature. The humidity would then become a computed dependent variable instead of an assigned parameter.

AIR-CONDITIONED ENCLOSURE PROBLEM

A two-room configuration was chosen for the enclosure to demonstrate the calculation of enclosure air motion, thermal comfort, and pollutant transport in a residential structure. A perspective of the enclosure is shown schematically in Figure 1. The overall enclosure measures 7.0 m in length, 4.3 m in width, and 2.4 m in height with an incomplete partition that divides the enclosure lengthwise into two rooms. The two rooms will be identified as front and rear, where the front room is distinguished by a window that measures 1.1 m in height and 1.8 m in width and is positioned 0.8 m above the floor. A curtain covers the window such that a gap of 0.15 m is created between the curtain and the window plane. Air is allowed to circulate in the curtain-window gap and infiltrate through the window plane. The enclosure partition is located 2.8 m from the rear wall and contains a doorway connecting the two rooms that measures 2.3 m in height and 0.9 m in width.

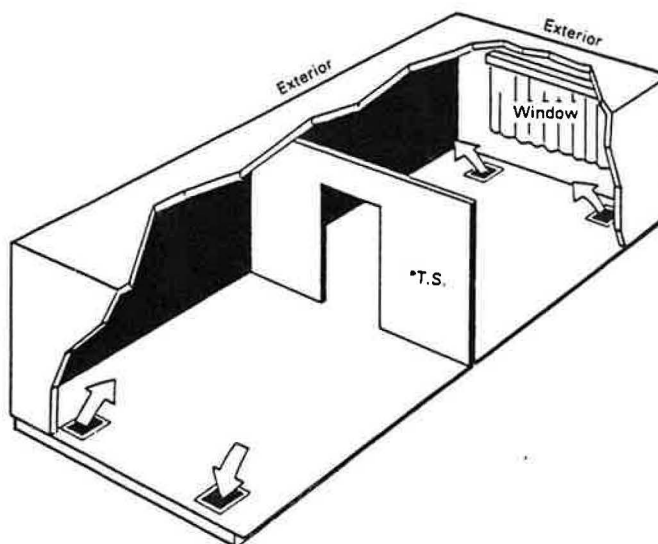


FIGURE 1. Partitioned Enclosure with Window

Four air circulation vents, two in each room, are located in the floor of the enclosure as indicated in Figure 1. Three of the vents supply forced air ventilation and the fourth serves as the return vent. The vent areas and ventilation flow rates are treated as parameters that are varied between the five simulations as outlined in Table 1 below. The turnover rates are volumetric air exchange rates computed based on continuous operation of the air circulation system. The actual turnover rates were problem dependent because the ventilation system was thermostatically controlled. For the first four simulations, the window and curtain were neglected. In the fifth simulation, the window was assigned an infiltration rate for hot air based on a 2 min cycle. The window infiltration rate linearly cycled between 2.5% and 7.5% of the continuous forced air ventilation rates. This infiltration model was designed to simulate a partially open window with a wind driven leakage.

TABLE 1. Simulation Log

Case	Vent Area	Air Velocity	Turnover Rate
1	0.046 m ²	0.305 m/s	2 hr ⁻¹
2	0.046 m ²	0.610 m/s	4 hr ⁻¹
3	0.093 m ²	0.305 m/s	4 hr ⁻¹
4	0.046 m ²	1.219 m/s	8 hr ⁻¹
4w	0.046 m ²	1.219 m/s	8.2 hr ⁻¹

The boundary conditions for the simulations were as follows: 1) constant floor temperature of 21.1°C, 2) constant ceiling temperature of 29.4°C, and 3) a constant linear gradient wall temperature varying from the floor to the ceiling temperatures. These boundary conditions were held constant throughout the calculations. The wall boundary conditions could have been modeled in a number of different ways, such as thermal conductors and capacitors subject to exterior ambient temperatures, or as adiabatic interior walls. The choice is user determinable for the problem under consideration. The conditions used here are consistent with an initially quiescent flow field, a stable thermally stratified environment, and relatively high heat capacitance walls, with elevated exterior temperatures.

Ventilation was thermostatically controlled with an "on-off" controller between the limits of 18.3°C and 23.9°C. The air-conditioned supply air was assigned a temperature of 15.6°C, and was controlled by a thermostat located at a height of 1.6 m on the rear room side of the partition wall as indicated in Figure 1. An air-conditioning problem was an arbitrary choice for the demonstration problem; the boundary and initial conditions could be modified to simulate heating

conditions for the same enclosure. The floor vents were chosen because effects of buoyancy, stratification, and ventilation air penetration are readily discernable.

The pollutant source was uniformly distributed over the ceiling region of the rear room with a source strength of 0.25 cc/s. This source strength is somewhat arbitrary and may not be typical. For the simulations investigated, however, it results in concentrations that are most dramatically affected by the phenomena of buoyancy, stratification, and forced ventilation.

RESULTS: CONVENTIONAL PRESENTATION

The results for the simulations numbered 1 to 4w are summarized with conventional time series plots of temperature and pollutant fractions, shown in Figures 2 to 6. Each figure is composed of two plots, the lower plot depicts four temperature histories and the upper plot four mass fraction histories. The four different lines on each plot represent the scalar value at four different positions throughout the enclosure. The dashed line depicts the response next to the ceiling in the front room above the doorway. The dash-dotted line depicts the response next to the ceiling in the front room above the window. The solid line depicts the response next to the ceiling in the rear room above the doorway. The dotted line depicts the response of the air around the thermostat.

The temperature and pollutant fraction responses shown for Case 1, represent a situation where the supply temperature and ventilation rates are insufficient to cause the system to cycle. The pollutant source strength was arbitrarily set excessively high for demonstration purposes. The solution, however, assumes a dilute pollutant strength regardless of computed concentration.

The ventilation systems of Cases 2 and 3 provided identical volumetric air turnover rates, which were sufficient to cause the system to cycle. The plots shown in Figures 3 and 4 span 2 hour periods that capture an entire cycle of the thermostat. The cycle period for Case 2 was slightly shorter than that for Case 3, because the higher ventilation flow velocities of Case 2 produced more homogeneous fields. This phenomenon can be observed in both the temperature and pollutant fraction plots. The ventilation flow rate for either simulation was, however, insufficient to disrupt the thermal stratification or dilute the pollutant concentrations near the ceiling in the front room. In fact, the pollutant

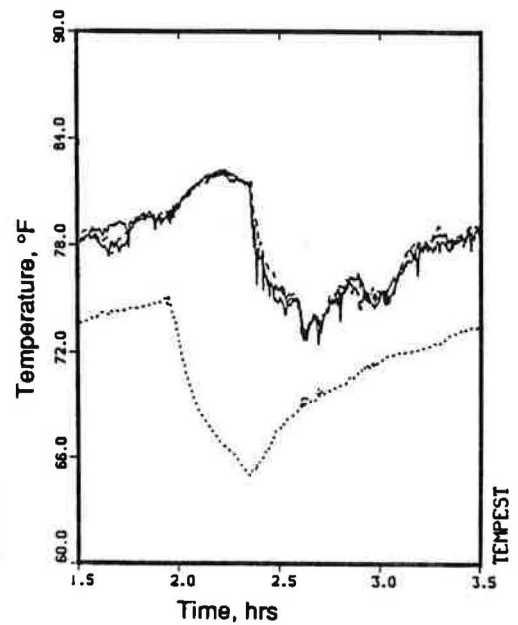
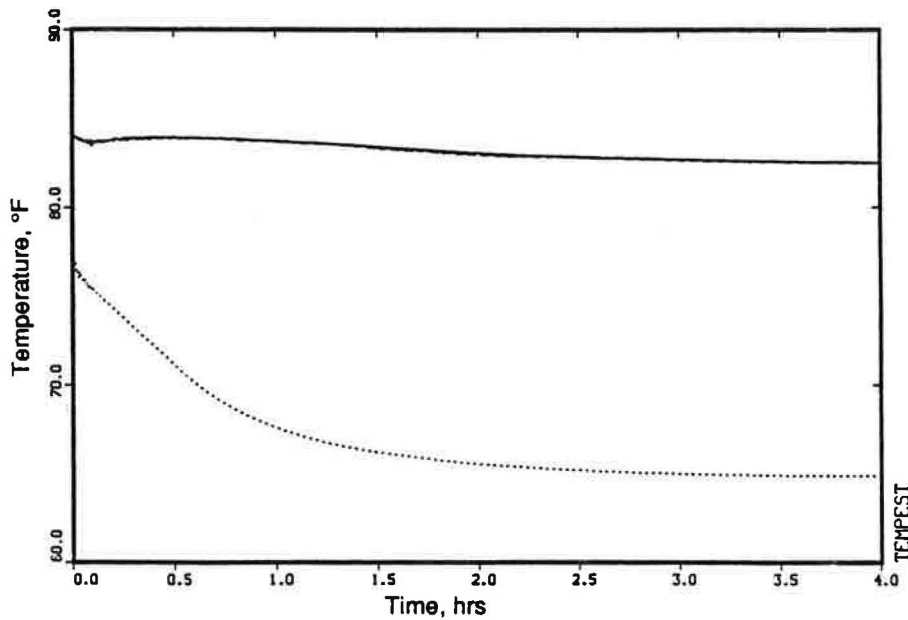
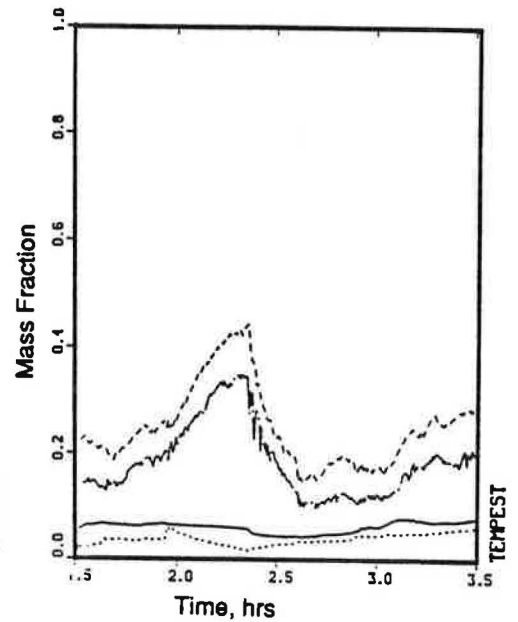
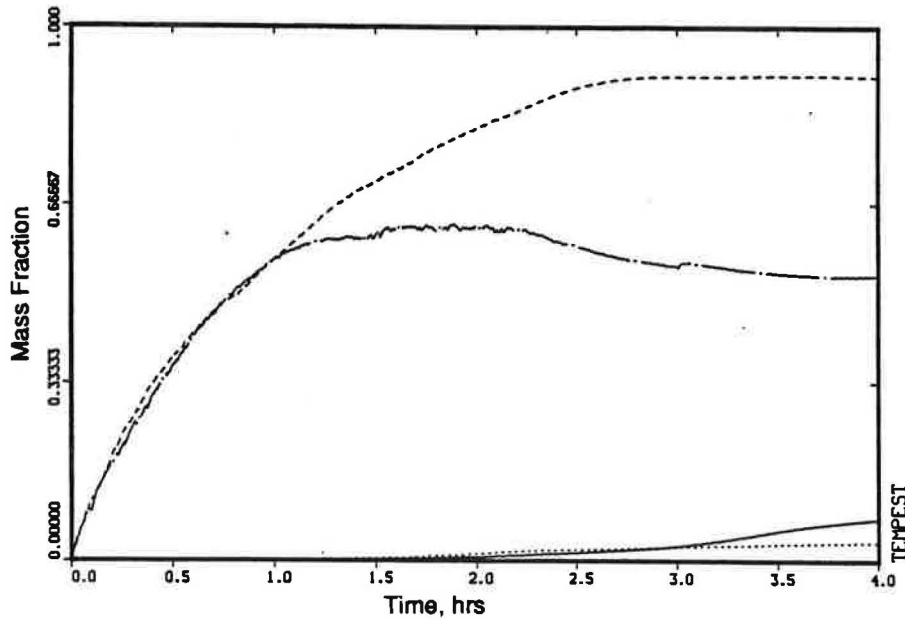


FIGURE 2. Case 1 Results

concentration near the ceiling in the locations plotted increased immediately following the ventilation system startup.

The simulation flow velocities and volumetric exchange rates for Cases 4 and 4w were sufficiently high to disrupt the thermal gradients and pollutant concentrations near the ceilings of both rooms. Both the temperature and mass fraction plots indicate a rapid decline in pollutant concentrations and temperatures following the ventilation system startup. In Case 4w the effect of the 2 min period cyclic window infiltration appeared as relatively low-amplitude wave of high frequency compared with the system cycle. These waves are easily observed in the mass fraction plot. As expected, the window

FIGURE 3. Case 2 Results

infiltration caused the ventilation system to cycle more frequently and produced greater swings in the ceiling temperatures.

GRAPHICS PRESENTATION TECHNIQUES

The graphics presentation techniques addressed were designed to be viewed on a high resolution color computer monitor connected to an interactive terminal. The interactive feature of the graphics presentation allows the viewer to examine simulation results with practically instantaneous view angle variations, and data switching. In lieu of an interactive computer terminal and monitor, the next most appropriate presentation media would be video tape recordings where the viewer would lose some

FIGURE 4. Cases 3 Results

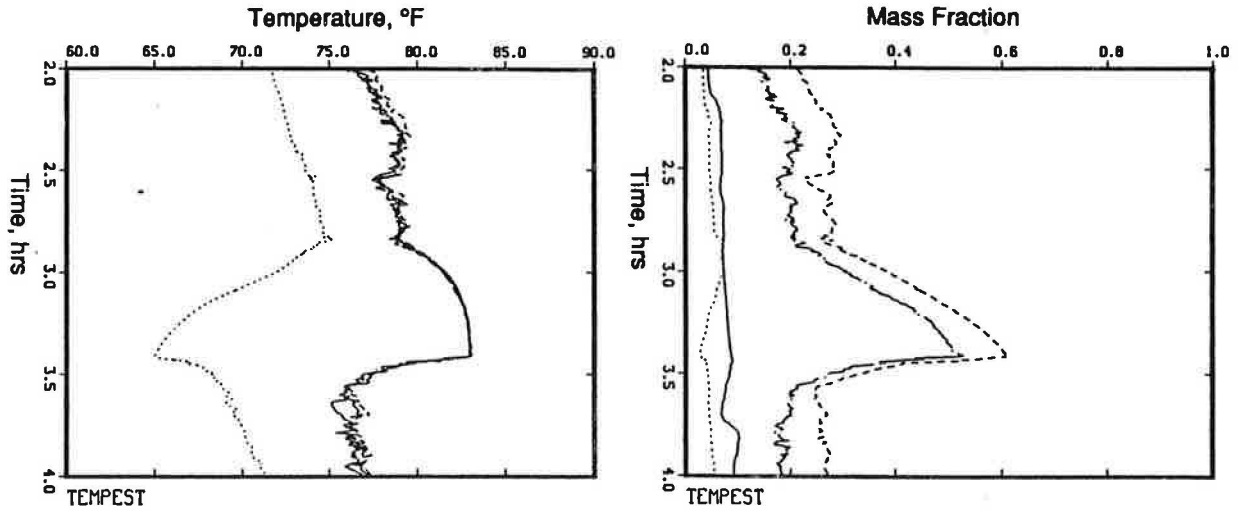


FIGURE 5. Case 4 Results

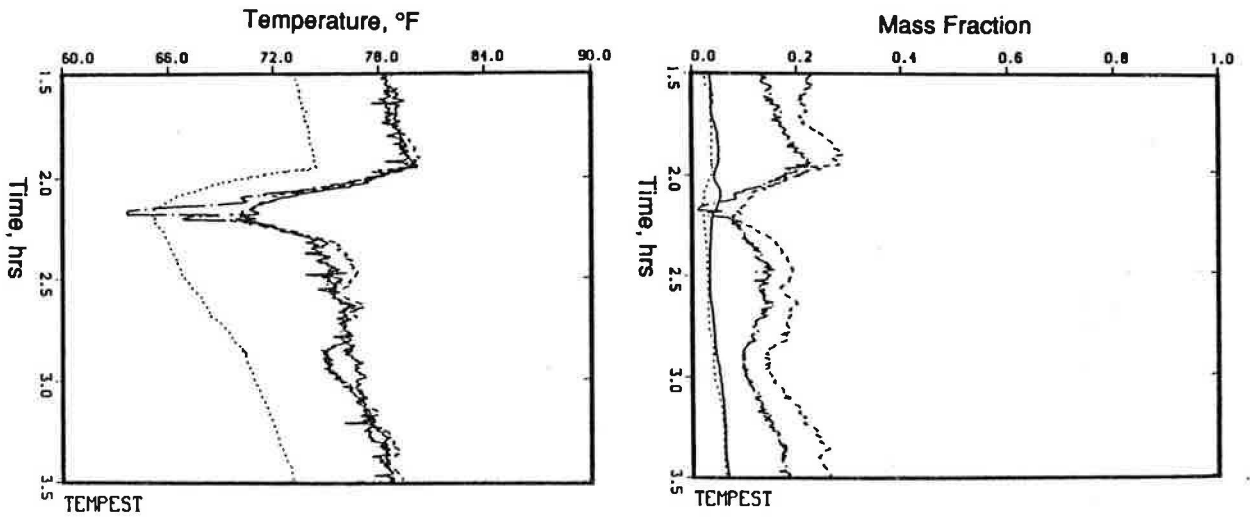
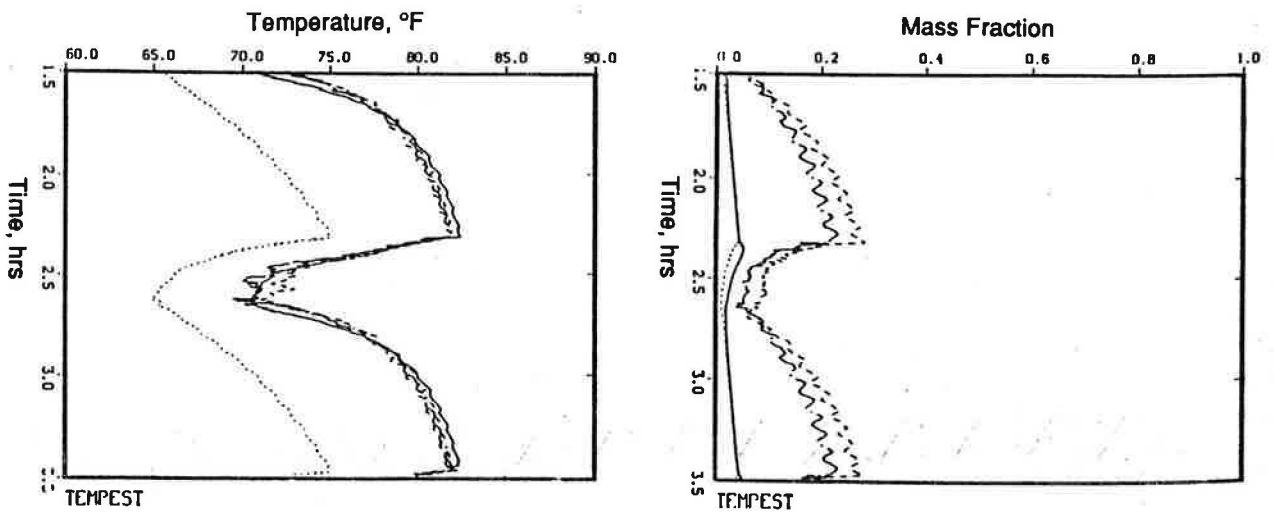


FIGURE 6. Case 4w Results



interactive features, but the capability for motion is retained. Of the popular media, color slides rank next in the descending order for graphics presentation techniques because the motion features have disappeared, but the color display is maintained. Unfortunately, the least appropriate media for graphics presentation is the black and white format of the printed page. Below we discuss the various visualization techniques and their merits and/or detriments. View rotation coupled with transparent walls were employed to improve the graphics presentation. Spatially dependent color scaling or coding, shading, and/or motion were used to enhance visual interpretation.

Low-Order Visualization

A field of dots color scaled to the selected scalar data (temperature, comfort index). In three dimensional view, this presentation is difficult to interpret on the two dimensional screen, i.e., depth perception is practically impossible.

Enhanced Visualization

A field of dots with a single arrow extending out in the direction of the velocity vector. Several possibilities exist for this visualization mode: 1) to enhance the interpretation of vector direction, for flow visualization, a light intensity gradient is applied along a vector's arrow shaft, 2) the arrow shaft is color scaled to a selected scalar, or 3) two scalars are incorporated with color scaling one as a cube at the base of the arrow and the other into the arrow shaft. The latter technique gives a five dimensional presentation with three components of velocity and two scalars. Whereas the human eye is a good "integrator," these approaches tend to overload the screen with information.

Motion Scaling

This approach attempts to present scalar information by degree of motion. The motion scaling included: 1) offsetting a velocity vector from its origin by a distance proportional to a scalar and rotating the vector about its origin, 2) rotating a velocity vector in a conical manner with the conical angle scaled to a scalar, 3) longitudinally vibrating a velocity vector with the oscillation amplitude scaled to a scalar, 4) scaling a scalar to the magnitude of an oscillating bar perpendicular to and at the base of a velocity vector. Motion scaling yields a rather innovative and intriguing presentation, but is complicated by the information overload and by the motion distortion caused by the viewing limitations of a flat screen.

Marker Balls

In this approach colored balls are selectively distributed within the flow field, where the ball color is coded by a local scalar value. The balls then proceed to move around the flow field according to the local velocity vector. As the balls migrate throughout the flow field, roughly 10 of each ball's most recent positions are displayed. The ball color varies with the local value of the selected scalar. Depth perception remains a problem with this approach and the balls tend to collect in low velocity regions. As with the other graphics techniques, however, the information is discernable.

Volume Segmenting

A rectangular volume of the entire computational domain is selected and the surfaces of the volume are color graduated according to a selected scalar. The volume may be rotated to view the scalar variation from all directions. With this approach the depth perception problem is no longer present, however, the technique is relatively time consuming if representation at the full computational domain is required.

Contour Surfaces

This approach involves forming a colored surface contour of a selected scalar. This contour surface can be shaded by an imaginary light source, which yields an image that appears three-dimensional. Moreover, the image may be viewed in "three-dimensions" with the aid of stereo projection; where the image is viewed through special polarizing lens. This presentation appears to be one of the more useful for viewing a scalar value over the entire volume. The surfaces generated for these scalar values can represent zones of comfort or pollutant levels. An example of a contour surface image is shown in Figure 7. The image shows a surface of constant comfort index equal to -0.898, for a simulation period with the ventilation system operating.

During the present investigation these graphics presentations were studied on a single static data fields of velocity, temperature, and comfort index. The presentation techniques, however, may be used in a dynamic mode, where successive frames of data from a transient problem are viewed in relatively rapid sequence. This dynamic mode would require some preconditioning of the data fields in terms of view angle, scalar selection, etc.; however, the end result would permit the viewing of time-dependent effects of the ventilation cycle, for example.

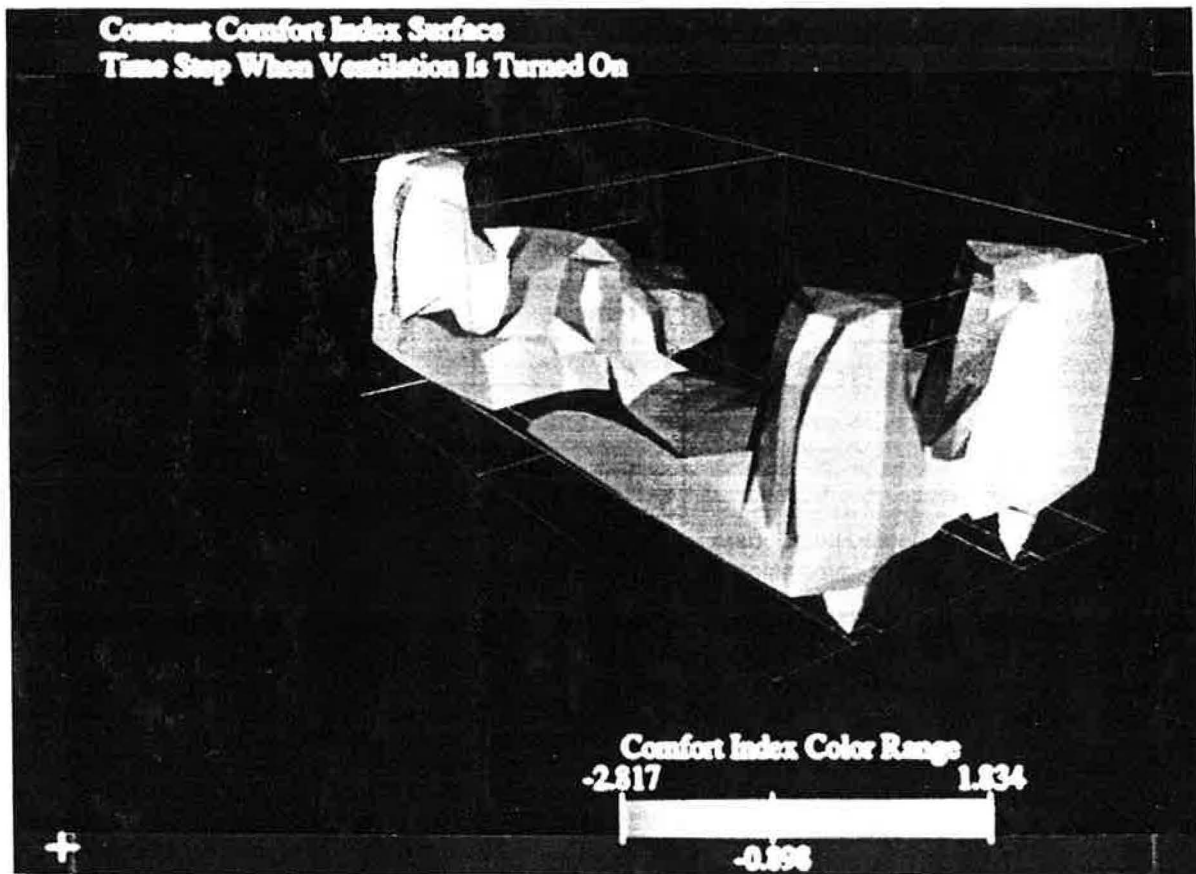


FIGURE 7. Constant Comfort Index Surface (-0.898)

CONCLUSIONS

The presentation of the results for the enclosure air-conditioning problem was not intended as a complete treatise on indoor air quality or thermal comfort for that particular building geometry. Rather the intent was to demonstrate the utility of computational fluid dynamics in conjunction with enhanced graphics presentation. A secondary aim of the paper was to investigate the utility of reducing the temperature, velocity, and humidity fields obtained from numerical models into a single scalar variable, the comfort index. We draw the following conclusions:

- The graphics presentation of computational fluid dynamic results applied to building sciences research and design can convey both rapid volume integral and detailed flow field data in a way that is rapidly understood.
- The comfort index results suggest that the single field of comfort index is an effective substitute to the multiple scalar and vector fields of temperature, humidity, and velocity.

- Indoor air quality issues concerned with pollutant transport can be practically and competently addressed with computational fluid dynamic techniques.

REFERENCES

- ASHRAE HANDBOOK 1985 Fundamentals. 1985. American Society of Heating, Refrigerating, and Air-Conditioning Engineers, Inc. New York, New York. (Chapter 8).
- Fanger, P. O. 1967. "Calculation of Thermal Comfort: Introduction of a Basic Comfort Equation." ASHRAE Transactions, Vol. 73, Part II, p. III.4.1.
- Fanger, P. O. 1970. Thermal Comfort. Analysis and Applications in Environmental Engineering. Danish Technical Press. Copenhagen, Denmark.
- Trent, D. S., L. L. Eyler, and M. J. Budden. 1969. TEMPEST - A Three-Dimensional Time-Dependent Computer Program for Hydrothermal Analysis. Volume 1: Numerical Methods and User Input. PNL-4348, Vol. 1, Rev. 2, Pacific Northwest Laboratory, Richland, Washington.